MRI Features of Renal Oncocytoma and Chromophobe Renal Cell Carcinoma

Andrew B. Rosenkrantz[1]
Nicole Hindman[1]
Erin F. Fitzgerald[1]
Benjamin E. Niver[1]
Jonathan Melamed[2]
James S. Babb[1]

OBJECTIVE. The purpose of this study was to retrospectively describe the MRI features of the pathologically related entities renal oncocytoma and chromophobe renal cell carcinoma (RCC).

MATERIALS AND METHODS. Twenty-eight cases of histologically proven renal oncocytoma and 15 of chromophobe RCC evaluated with preoperative MRI from January 2003 through June 2009 at our institution were independently reviewed for an array of MRI features by two radiologists blinded to the final histopathologic diagnosis. These features were tabulated and compared between chromophobe RCC and renal oncocytoma by use of the Mann-Whitney test and binary logistic regression.

RESULTS. Renal oncocytoma and chromophobe RCC showed no significant difference in size or any of 16 qualitative imaging features (p = 0.0842–1.0, reader 1; p = 0.0611–1.0, reader 2). Microscopic fat, hemorrhage, cysts, infiltrative margins, perinephric fat invasion, renal vein invasion, enhancement homogeneity, and hypervascularity were each observed in less than 20% of cases by both readers. A central scar and segmental enhancement inversion (a recently described finding in which early contrast-enhanced images show relatively more enhanced and less enhanced intralesional components with inversion of their relative enhancement on later images) were observed by both readers in at least 10% of cases of both renal oncocytoma and of chromophobe RCC with no significant difference between the two entities (p = 0.2092–0.2960).

CONCLUSION. We have presented the largest series to date of the MRI features of both renal oncocytoma and chromophobe RCC. These related entities exhibited similar findings, and no MRI features were reliable in distinguishing between them.

Keywords: central scar, chromophobe renal cell carcinoma, MRI, renal mass, renal oncocytoma

DOI:10.2214/AJR.10.4718

Received April 1, 2010; accepted after revision May 22, 2010.

[1]Department of Radiology, New York University Langone Medical Center, 560 First Ave., TCH-HW202, New York, NY 10016. Address correspondence to A. B. Rosenkrantz (Andrew.Rosenkrantz@nyumc.org).

[2]Department of Pathology, New York University Langone Medical Center, New York, NY.

WEB
This is a Web exclusive article.

AJR 2010; 195:W421–W427

0361–803X/10/1956–W421

Renal oncocytoma is the second most common benign renal neoplasm after angiomyolipoma, comprising 3–7% of all renal tumors. Chromophobe renal cell carcinoma (RCC) is the third most common histologic subtype of RCC after the clear cell and papillary subtypes, comprising approximately 6–8% of all renal tumors and approximately 4–10% of all cases of RCC [1]. These two entities differentiate toward the intercalated cells of the collecting duct system and share morphologic, histologic, immunohistochemical, and ultrastructural features [2]. Despite this considerable overlap in pathologic features, the two entities can be reliably distinguished at pathologic examination in most cases [3, 4], and the distinction can affect clinical management. Renal oncocytoma is generally considered a benign lesion. Chromophobe RCC, although having a more favorable prognosis than other RCC subtypes, is a malignant tumor with the potential for metastatic spread and death [1, 5].

Numerous studies have been conducted to identify imaging features for differentiating renal oncocytoma from RCC. These studies have generally been performed with CT, and a typical imaging appearance of renal oncocytoma has been set forth as a well-circumscribed homogeneous lesion, aside from a central stellate scar, with an absence of necrosis and hemorrhage [6–8]. Although the presence of the central scar can be characteristic of renal oncocytoma, it is not diagnostic. For instance, although Cochand-Priollet et al. [3] observed a fibrous scar in 45% of cases of renal oncocytoma at histologic analysis, these observers also observed a scar in 23% of cases of chromophobe RCC [3]. Renal malignancies can not only have a true fibrous scar, they also can exhibit necrosis at imaging that mimics the presence of a scar, further limiting the utility of this im-

aging finding for reliable identification of renal oncocytoma [9]. Kim et al. [10] observed a newly described imaging finding at biphasic CT, described as segmental enhancement inversion, in which corticomedullary phase images show components of relatively greater and less enhancement in a renal mass, and early excretory phase images show inversion of these relative intensities. In that study, segmental enhancement inversion was identified in eight of 10 cases of renal oncocytoma and one of 88 cases of RCC and was therefore deemed a characteristic imaging finding of renal oncocytoma. The one case of RCC in the series to exhibit segmental enhancement inversion was chromophobe RCC, which those investigators attributed to the similar histopathologic features of renal oncocytoma and chromophobe RCC.

MRI offers excellent soft-tissue contrast and is able to assess for the presence of specific histologic components, such as lipid and blood products. The role of MRI in accurate detection and staging of renal lesions has been well documented [11–13]. MRI also may serve a role in characterizing renal lesions given that specific MRI features have been found to correlate well with renal lesions of a distinct histologic composition, including clear cell RCC, papillary RCC, and renal angiomyolipoma [14–16]. This ability is important in view of the increasing incidental detection of small renal masses [17] and the expanding array of management options for such lesions, including partial nephrectomy, cryoablation, radiofrequency ablation, and active surveillance [18].

Despite increasing recognition of the role of MRI in the characterization of renal masses, the MRI features of renal oncocytoma and chromophobe RCC have not been fully characterized. To our knowledge, the largest series to describe the MRI features of renal oncocytoma was 11 cases reported by Harmon et al. [19] in 1996 and of chromophobe RCC was seven cases reported by Kondo et al. [20] in 2004, both studies being limited by small sample size. In addition, to our knowledge, no joint assessment has been performed of the imaging appearances of these two related entities, which may be expected to have overlapping imaging findings in view of their shared pathologic characteristics. Therefore, the purpose of our study was to retrospectively describe the MRI features of renal oncocytoma and chromophobe RCC with the hypothesis that there is no significant difference between the MRI features of these two entities.

Materials and Methods

Patients

This retrospective study was HIPAA compliant and approved by our institutional review board with waiver of informed consent. The pathology and radiology databases at our institution were searched to identify all cases of histologically proven chromophobe RCC and renal oncocytoma in which the patient had undergone preoperative MRI from January 2003 through June 2009. The search identified a total of 41 patients (mean age, 67 ± 14 years) who had a total of 43 tumors: 15 chromophobe RCC and 28 renal oncocytoma. One patient had three separate lesions (all renal oncocytoma). Cases were excluded if the pathology report indicated either coexistence of chromophobe RCC and renal oncocytoma in a single lesion (two cases) or uncertainty about the specific diagnosis (four cases).

MRI Technique

All patients underwent MRI with one of three clinical 1.5-T systems (Magnetom Avanto, Sonata, or Symphony, Siemens Healthcare) and a torso phased-array coil (six-element anterior and posterior coil arrays for the Avanto unit, four-element anterior and posterior coil arrays for the Sonata and Symphony units). Examinations included the following unenhanced sequences: axial and/or coronal HASTE (TR/TE_{eff}, 780–1,200/62–98; field of view, 263–500 × 325–500 mm; matrix size, 192–329 × 256–384; slice thickness, 4–6 mm; receiver bandwidth, 380–790 Hz/voxel; number of signals averaged, 1; no parallel imaging; 1–2 breath-holds of up to 25 seconds), axial in- and out-of phase 2D gradient-echo T1-weighted images ($TR/TE_1/TE_2$, 160–255/2.0–2.7/4.4–5.0; field of view, 263–366 × 325–450 mm; matrix size, 112–208 × 256; slice thickness, 6–8 mm; number of signals averaged, 1; with or without generalized autocalibrating partially parallel acquisition (GRAPPA) factor of 2; single breath-hold of up to 25 seconds), and 3D fat-suppressed gradient-echo T1-weighted images (TR/TE 3.1–4.5/1.2–1.9; field of view, 241–372 × 241–372 mm; matrix size, 104–177 × 256; slice thickness, 2–3 mm; number of signals averaged, 1; with or without GRAPPA factor of 2; single breath-hold of up to 25 seconds).

In all examinations, the 3D gradient-echo T1-weighted sequences were performed in a dynamic manner after administration of either 0.1 mmol/kg of gadopentetate dimeglumine (Magnevist, Bayer HealthCare) (39 patients) or 0.05 mmol/kg of gadobenate dimeglumine (MultiHance, Bracco Diagnostics) (two patients). Our department policy regarding nephrogenic systemic fibrosis determined which contrast agent was administered to each patient. The contrast agent was administered as an IV bolus through a power injector (Spectris, Medrad) followed by a 20-mL saline flush. Both the contrast bolus and the flush were administered at a rate of 2 mL/s. Contrast-enhanced sequences were performed in the corticomedullary, nephrographic, and excretory phases. The corticomedullary phase was timed to the arterial phase, determined as the time to peak enhancement of the abdominal aorta at the level of the renal arteries after injection of a 1-mL test bolus of IV contrast material followed by a 20-mL saline flush, both administered at a rate of 2 mL/s. Acquisition in the nephrographic and excretory phases was begun 1 minute and 3 minutes after the start of acquisition in the corticomedullary phase.

Imaging Analysis

All images were reviewed independently by two radiologists (2 and 4 years of experience in interpretation of abdominal MR images). These two reviewers were blinded to the histologic diagnoses of the lesions at the time of their review. The readers recorded the size of each lesion as its single greatest diameter in the axial plane and evaluated each lesion for the presence of each of the following 16 features: peripheral location (lesion contacts the outer margin of the kidney, with center of lesion in the renal cortex), microscopic lipid (area of signal loss in the lesion on out-of-phase T1-weighted images), hemosiderin (area of signal loss in the lesion on in-phase T1-weighted images), subacute hemorrhage (area of increased T1 signal intensity on unenhanced fat-suppressed T1-weighted images), T2 hyperintensity (relative to normal renal cortex), T2 signal homogeneity, cystic component, enhancement homogeneity, hypervascularity during the corticomedullary phase (relative to renal cortex), hypervascularity during the nephrographic phase (relative to renal cortex), hypervascularity during the excretory phase (relative to renal cortex), central scar (central stellate area of T2 hyperintensity with lack of enhancement during the corticomedullary phase with or without enhancement during subsequent phases), segmental enhancement inversion (based on definition and sample illustrations provided by Kim et al. [10]), infiltrative morphology (most of lesion having lack of well-defined margins with surrounding renal parenchyma), perinephric fat invasion (lesion containing an exophytic component with irregular margins with perinephric fat), and renal vein invasion.

Statistical Analysis

An exact Mann-Whitney test was used to compare chromophobe RCC and renal oncocytoma in terms of mean lesion size. Generalized estimating equations based on a binary logistic regression model were used to determine whether lesion type (chromophobe RCC or renal oncocytoma) was associated with any of the individual binary factors. In this context, stepwise variable selection was

performed to identify whether the combination of two or more of the aforementioned imaging features represented a significant independent predictor of malignancy (chromophobe RCC). These tests were performed separately for each reader. Correlation between the lesion sizes obtained by the two readers was assessed with Pearson's correlation coefficient. The concordance between readers for each of the binary factors was also determined, calculated for each factor as the percentage of lesions for which the two readers provided the same score. Kappa coefficients were not used for this determination because the very high prevalence of certain imaging features for many of the binary factors was expected to produce misleadingly low values [21]. To satisfy the assumption of independent observations underlying the Mann-Whitney and Pearson's tests, for the one patient with three lesions (all renal oncocytoma), lesion size was represented as the average size of the three individual lesions. All reported *p* values are two-sided and considered statistically significant when less than 0.05. SAS version 9.0 software (SAS Institute) was used for all computations.

Results

Lesions

A total of 43 lesions in 41 patients were included in the statistical analysis. These were 28 renal oncocytomas and 15 chromophobe RCCs. The mean lesion size was 3.4 ± 2.4 cm for reader 1 and 3.2 ± 2.5 cm for reader 2. The mean delay between MRI and surgery was 37 ± 24 days. The final histologic diagnosis was obtained by radical nephrectomy (10 lesions), partial nephrectomy (32 lesions), and core biopsy (one lesion).

TABLE 1: Comparison of Size of Renal Oncocytoma and Chromophobe Renal Cell Carcinoma

Lesion Type	Reader 1	Reader 2
Renal oncocytoma	3.51 ± 1.86	3.19 ± 1.99
Chromophobe renal cell carcinoma	3.35 ± 3.27	3.27 ± 3.30
p	0.2178	0.5421

Note—Values are mean ± SD in centimeters.

Imaging Features

The mean sizes of renal oncocytoma and chromophobe RCC were similar for the two readers with no statistically significant difference between the sizes of these lesions for reader 1 ($p = 0.2178$) or reader 2 ($p = 0.5421$) (Table 1). There was no statistically significant difference between renal oncocytoma and chromophobe RCC for any of the 16 assessed binary imaging features for either reader 1 ($p = 0.0842$–1.0) or reader 2 ($p = 0.0611$–1.0) (Table 2). In addition, stepwise multivariate logistic regression analysis failed to identify any combination of two or more measures that was able to serve as a significant predictor of the presence of malignancy (chromophobe RCC).

Both readers scored a number of the assessed imaging features in the same way in at least 80% of cases of both renal oncocytoma and chromophobe RCC (Table 2). Specifically, at least 80% of cases of renal oncocytoma and chromophobe RCC had a peripheral location and lacked the following features: microscopic fat, subacute hemorrhage, cysts, enhancement homogeneity, corticomedullary phase hyperintensity, nephrographic phase hyperintensity, excretory phase hyperintensity, and perinephric fat invasion. Furthermore, in all cases, both renal oncocytoma and chromophobe RCC lacked infiltrative margins and renal vein invasion. Hemosiderin was absent in more than 80% of cases of both renal oncocytoma and chromophobe RCC, aside from

TABLE 2: Frequency of Assessed Qualitative Imaging Features in Renal Oncocytoma and Chromophobe Renal Cell Carcinoma

	Reader 1			Reader 2		
Feature	Renal Oncocytoma	Chromophobe Renal Cell Carcinoma	*p*	Renal Oncocytoma	Chromophobe Renal Cell Carcinoma	*p*
Peripheral location	92.9 (26/28)	86.7 (13/15)	0.5133	96.4 (27/28)	86.7 (13/15)	0.2635
Microscopic fat	0.0 (0/28)	6.7 (1/15)	0.9567	0.0 (0/28)	0.0 (0/15)	1.0
Subacute hemorrhage	3.6 (1/28)	20.0 (3/15)	0.1143	0.0 (0/28)	6.7 (1/15)	0.9567
Hemosiderin	7.1 (2/28)	6.7 (1/15)	0.9536	14.3 (4/28)	26.7 (4/15)	0.3306
T2 hyperintensity	46.4 (13/28)	40.0 (6/15)	0.6979	50.0 (14/28)	40.0 (6/15)	0.5461
T2 homogeneity	25.0 (7/28)	33.3 (5/15)	0.5679	14.3 (4/28)	33.3 (5/15)	0.1568
Cysts	14.3 (4/28)	0.0 (0/15)	0.2804	10.7 (3/28)	20.0 (3/15)	0.4118
Enhancement homogeneity	10.7 (3/28)	33.3 (5/15)	0.0842	0.0 (0/28)	26.7 (4/15)	0.0611
Corticomedullary phase hyperintensity	0.0 (0/28)	6.7 (1/15)	0.9567	3.6 (1/28)	13.3 (2/15)	0.2635
Nephrographic phase hyperintensity	0.0 (0/28)	0.0 (0/15)	1.0	3.6 (1/28)	6.7 (1/15)	0.6517
Excretory phase hyperintensity	0.0 (0/28)	0.0 (0/15)	1.0	7.1 (2/28)	0.0 (0/15)	0.5354
Central scar	50.0 (14/28)	33.3 (5/15)	0.2920	60.7 (17/28)	40.0 (6/15)	0.2092
Segmental enhancement inversion	28.6 (8/28)	13.3 (2/15)	0.2640	42.9 (12/28)	26.7 (4/15)	0.2960
Infiltrative margins	0.0 (0/28)	0.0 (0/15)	1.0	0.0 (0/28)	0.0 (0/15)	1.0
Perinephric fat invasion	10.7 (3/28)	6.7 (1/15)	0.6671	14.3 (4/28)	6.7 (1/15)	0.4697
Renal vein invasion	0.0 (0/28)	0.0 (0/15)	1.0	0.0 (0/28)	0.0 (0/15)	1.0

Note—Values are percentage with raw numbers in parentheses. No imaging feature had a statistically significant difference between renal oncocytoma and chromophobe renal cell carcinoma at $p < 0.05$.

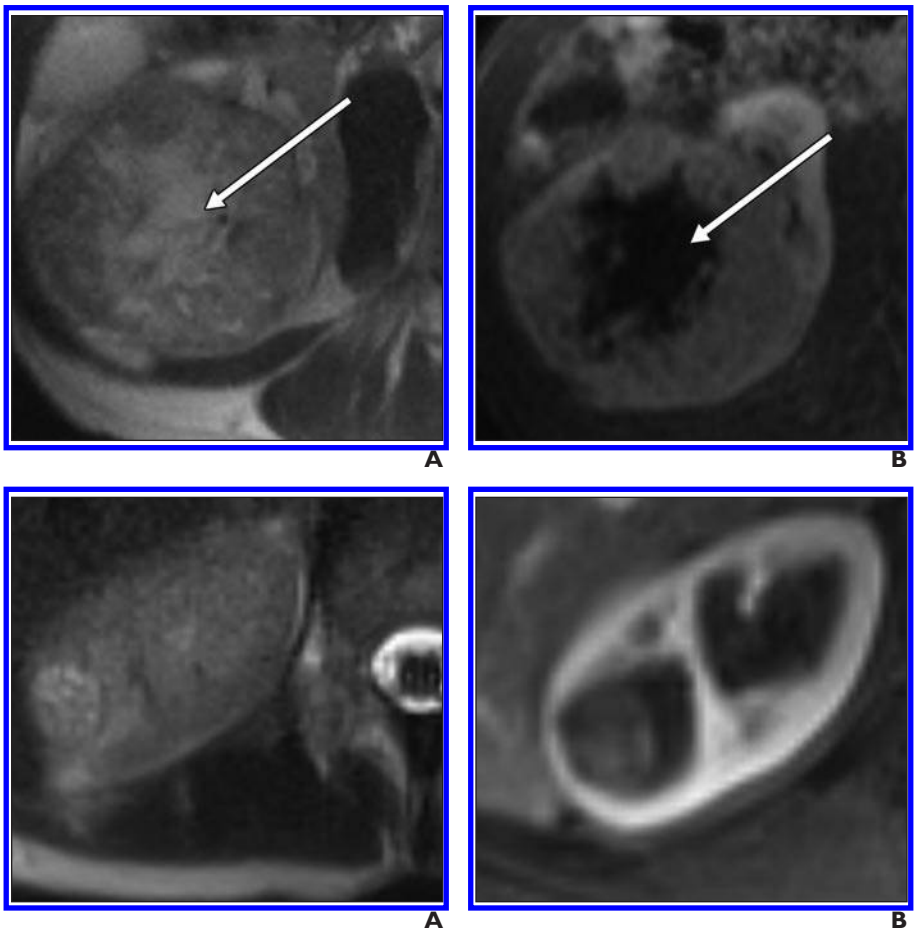

Fig. 1—81-year-old woman with pathologically proved chromophobe renal cell carcinoma. **A** and **B,** Axial HASTE (**A**) and axial excretory phase 3D gradient-echo T1-weighted (**B**) MR images show predominantly well-circumscribed mass with large central scar (*arrow*) and peripheral heterogeneous solid component that is hypointense relative to renal cortex in **B**.

Fig. 2—56-year-old woman with pathologically proved chromophobe renal cell carcinoma. **A** and **B,** Axial HASTE (**A**) and axial corticomedullary phase 3D gradient-echo T1-weighted (**B**) MR images show well-circumscribed mass of heterogeneous T2 signal intensity and enhancement that is predominantly hyperintense to renal cortex in **A** and hypointense in **B**. No central scar or segmental enhancement inversion was detected.

being scored as present in 26.7% of cases of chromophobe RCC by reader 2. Both renal oncocytoma and chromophobe RCC lacked T2 homogeneity in at least 60% of cases for both readers. Finally, central scar and segmental enhancement inversion were observed among cases of both renal oncocytoma and chromophobe RCC as follows: A central scar was seen in 50.0% and 33.3% of cases of renal oncocytoma and chromophobe RCC by reader 1 and in 60.7% and 40.0% of cases of renal oncocytoma and chromophobe RCC by reader 2. Segmental enhancement inversion was seen in 28.6% and 13.3% of cases of renal oncocytoma and chromophobe RCC by reader 1 and in 42.9% and 26.7% of cases by reader 2 (Figs. 1–4).

Reader Concordance

There was highly significant correlation between the two readers in terms of lesion size ($r = 0.98$, $p < 0.0001$). In addition, concordance of the two readers for each of the assessed binary features was very good to excellent, ranging from 79.1% to 100.0% for all features (Table 3).

Discussion

To our knowledge, our study was the first joint assessment of the imaging features of the related diagnoses renal oncocytoma and chromophobe RCC as well as the largest series to date to describe the MRI features for both of these entities. Both renal oncocytoma and chromophobe RCC tended to appear on MR images as localized peripheral masses that were hypovascular compared with renal cortex in all phases of contrast enhancement. None of the MRI features assessed showed a significant difference between these two entities for either radiologist.

Renal oncocytoma and chromophobe RCC originate from a common progenitor cell in the kidney and have overlapping histologic features [22, 23]. Careful assessment with incorporation of a number of pathologic features allows accurate pathologic differentiation of these entities in most cases. This distinction may be important in the care of patients whose condition does not allow surgical treatment, who have renal dysfunction, or who have multiple renal masses [9, 19]. Numerous case series [1, 4, 5] describe small rates of postoperative recurrence, metastatic disease, and mortality from chromophobe RCC. Renal oncocytoma, however, is a benign lesion. Nearly all cases of metastatic renal oncocytoma reported in the literature are currently believed to have in fact represented metastatic chromophobe RCC. The single pathologically proven case of metastasis from renal oncocytoma was a hepatic metastatic lesion that was stable after 58 months of follow-up [22–24].

Imaging features common to renal oncocytoma and chromophobe RCC in our study included peripheral location, completely or predominantly well-circumscribed margins, and lack of perinephric fat invasion or renal vein invasion. These features are compatible with the benignity of renal oncocytoma and the generally low stage and indolent behavior of chromophobe RCC. In addition, both renal oncocytoma and chromophobe RCC were most often hypovascular relative to renal cortex at each of the assessed phases of dynamic contrast-enhanced imaging. Hypovascularity, although variably defined across studies, has been observed for renal onco-

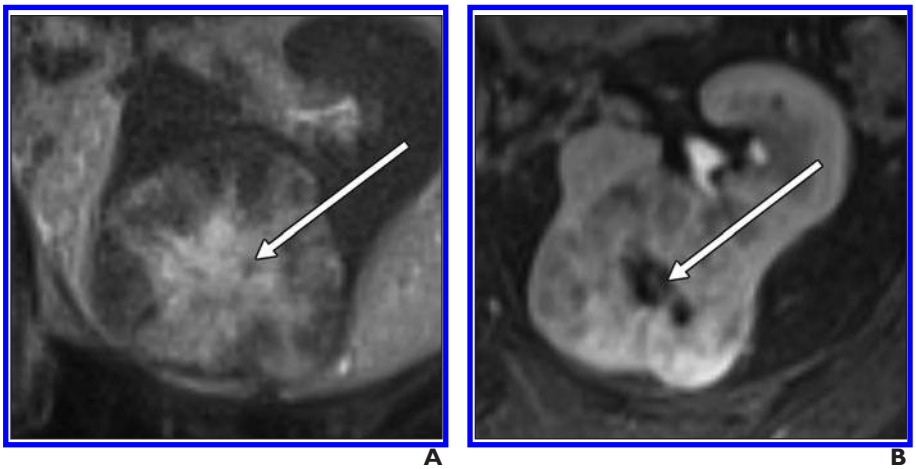

Fig. 3—68-year-old man with pathologically proved oncocytoma.
A and **B,** Axial HASTE (**A**) and axial nephrographic phase 3D gradient-echo T1-weighted (**B**) MR images show predominantly well-circumscribed mass with central scar (*arrow*) and peripheral heterogeneous solid component that is hypointense relative to renal cortex in **B**.

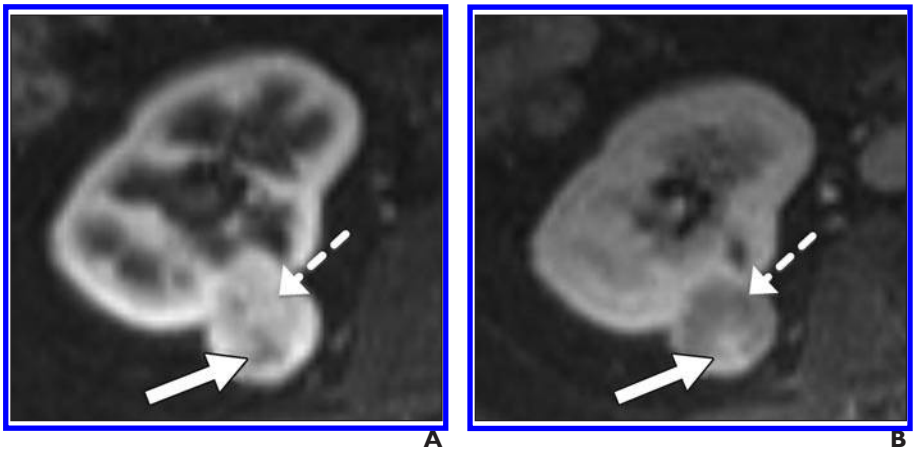

Fig. 4—58-year-old man with pathologically proved oncocytoma.
A and **B,** Axial corticomedullary (**A**) and nephrographic phase 3D gradient-echo T1-weighted (**B**) MR images show well-circumscribed mass in posterior aspect of right kidney. Enhancement pattern whereby posterior area is less enhanced (*solid arrow*) and anterior area is more enhanced (*dashed arrow*) in **A** is inverted in **B**.

cytoma in numerous CT studies and reported for a small series of chromophobe RCC evaluated with MRI [7, 20, 25–27]. In comparison, hyperenhancement relative to renal cortex during the corticomedullary phase that becomes less marked during the nephrographic phase is characteristic of clear cell RCC [25], which has been found in multivariate analysis to be associated with worse outcome than chromophobe RCC [28].

In our study, both renal oncocytoma and chromophobe RCC most often had heterogeneous T2 signal intensity and enhancement. In comparison, both of these lesions have been described in previous CT studies as typically having a homogeneous appearance [6, 7, 26]. However, all six cases of chromophobe RCC detected with MRI in the series by Kondo et al. [20] were described as heterogeneous. It is possible that owing to the superior soft-tissue contrast of MRI, MRI may have greater sensitivity than CT to the heterogeneous composition of these lesions.

We assessed all lesions for the presence of a central scar and segmental enhancement in-

TABLE 3: Comparison of Concordance Between Readers for Each Assessed Qualitative Imaging Feature

Attribute	Concordance
Peripheral location	97.7 (42/43)
Microscopic fat	97.7 (42/43)
Hemorrhage	93.0 (40/43)
Hemosiderin	88.4 (38/43)
T2 hyperintensity	88.4 (38/43)
T2 homogeneity	79.1 (34/43)
Cysts	81.4 (35/43)
Enhancement homogeneity	90.7 (39/43)
Corticomedullary phase hyperintensity	90.7 (39/43)
Nephrographic phase hyperintensity	95.3 (41/43)
Excretory phase hyperintensity	95.3 (41/43)
Central scar	81.4 (35/43)
Segmental enhancement inversion	81.4 (35/43)
Infiltrative margins	100.0 (43/43)
Perinephric fat invasion	97.7 (42/43)
Renal vein invasion	100.0 (43/43)

Note—Values are percentages with raw numbers in parentheses.

version. Although these imaging findings have been described as suggestive of renal oncocytoma, caution is warranted because RCC can exhibit a central scar, and segmental enhancement inversion has been assessed only in one study as of this writing, to our knowledge. In our study, the frequency of these findings ranged from 13.3% to 60.7% when the assessments of both groups of lesions by both readers were considered. The stellate scar observed on imaging corresponds to the coalescent central bands of fibrosis and compressed blood vessels that have been described as histologic findings in both renal oncocytoma and chromophobe RCC [3, 4, 16, 24, 29]. Segmental enhancement inversion is postulated to reflect areas of variable hyalinized stromal content in which tumor cells are embedded [10]. It is possible that the presence of either of these two imaging findings favors a diagnosis of either renal oncocytoma or chromophobe RCC over other renal lesions without specifically favoring one or the other of these two diagnostic possibilities. The lack of a significant difference between renal oncocytoma and chromophobe RCC with respect to the frequency of either of these two findings.

Cysts, subacute hemorrhage, hemosiderin, and microscopic lipid all tended to be observed very rarely in either renal oncocytoma or chromophobe RCC. At histologic analysis, Cochand-Priollet et al. [3] similarly observed cystic areas and hemorrhage in a small proportion of cases of both renal oncocytoma and chromophobe RCC and found no significant difference between the two lesions with respect to the frequency of these findings. Microscopic lipid is typically associated with clear cell RCC [16], and the observation of this finding in one case of chromophobe RCC by one of the two readers was unexpected. Krishnan et al. [30], however, did note that a scant amount of lipid was present at electron microscopic analysis of some cases of renal oncocytoma and chromophobe RCC.

We found no significant difference between the mean lesion size of renal oncocytoma and chromophobe RCC. This lack of difference in size concurs with a similar observation on these two entities in the pathology literature [3]. Although some studies have shown an association between lesion size and natural history of renal masses [31, 32], small size alone is not sufficient to warrant conservative management given that lesion size by itself is not a reliable predictor of malignancy [33, 34].

An ability to confidently diagnose renal oncocytoma preoperatively may be valuable in facilitating conservative management in the appropriate clinical setting. However, studies that have suggested imaging features that can be used to make this diagnosis have been limited by small sample size and generally have assessed renal oncocytoma in isolation or in comparison with all histologic subtypes of RCC [7, 19]. Although chromophobe RCC is an uncommon subtype of RCC, it is this subtype that is most likely to cause confusion with renal oncocytoma in attempts to establish a preoperative diagnosis [4, 23]. Our findings regarding overlapping imaging features of renal oncocytoma and chromophobe RCC may be useful in a scenario in which conservative management would be considered for a diagnosis of either chromophobe RCC or renal oncocytoma. Despite its potential for metastatic spread, chromophobe RCC is considered to have low malignant potential given that the tumors have indolent biologic behavior and remain confined to the kidney in most cases, thereby having a better overall prognosis than other subtypes of RCC [1, 28]. For instance, Thoenes et al. [5] and Crotty et al. [4] each estimated a survival rate greater than 90% for chromophobe RCC. Therefore, in a highly select patient population, it is conceivable that simply identifying that a renal mass likely represents either renal oncocytoma or chromophobe RCC on the basis of MRI findings, without differentiating these two possibilities, may influence management.

Our study had limitations. First, the retrospective nature likely introduced selection basis. Second, because no other renal lesions were evaluated, our results do not indicate the specificity of any of the findings we assessed for the presence of renal oncocytoma or chromophobe RCC relative to other benign and malignant renal lesions. Third, the imaging findings were assessed in a qualitative manner. However, the concordance between the two readers ranged from very good to excellent for all of the assessed parameters. Fourth, given the low frequency of chromophobe RCC, we included images acquired over a period longer than 6 years, and the sequence parameters of our routine renal protocol changed during this time. Fifth, the statistical power to identify significant differences between chromophobe RCC and renal oncocytoma with respect to the frequency of individual MRI features was low given the sample size in this study. Therefore, it is possible that there were differences between the MRI features of the two groups that our study lacked the statistical power to detect. Finally, the presence of hybrid renal lesions that contain an admixture of areas of renal oncocytoma and chromophobe RCC is an increasingly recognized entity for which the biologic and clinical significance is not currently known [22, 23, 35]. We excluded all such lesions and therefore were unable to make conclusions regarding the imaging appearance of this entity.

In conclusion, we have presented the largest series, to our knowledge, to jointly describe the MRI features of renal oncocytoma and chromophobe RCC. The similar imaging findings exhibited by these two entities are concordant with their overlapping pathologic features. Both of these lesions appeared as localized well-circumscribed masses that were hypovascular relative to renal cortex in all phases of contrast enhancement. A number of features, such as cysts, microscopic lipid, subacute hemorrhage, and hemosiderin, were uncommon for both lesions. Central scar and segmental enhancement inversion, imaging features that have been described as suggestive of renal oncocytoma in limited contexts, were observed in a similar proportion of the two lesions. No MRI features were reliable for differentiating these two entities, and histologic examination remains necessary for establishing either diagnosis.

References

1. Amin MB, Paner GP, Alvarado-Cabrero I, et al. Chromophobe renal cell carcinoma: histomorphologic characteristics and evaluation of conventional pathologic prognostic parameters in 145 cases. *Am J Surg Pathol* 2008; 32:1822–1834
2. Tickoo SK, Amin MB. Discriminant nuclear features of renal oncocytoma and chromophobe renal cell carcinoma: analysis of their potential utility in the differential diagnosis. *Am J Clin Pathol* 1998; 110:782–787
3. Cochand-Priollet B, Molinie V, Bougaran J, et al. Renal chromophobe cell carcinoma and oncocytoma: a comparative morphologic, histochemical, and immunohistochemical study of 124 cases. *Arch Pathol Lab Med* 1997; 121:1081–1086
4. Crotty TB, Farrow GM, Lieber MM. Chromophobe cell renal carcinoma: clinicopathological features of 50 cases. *J Urol* 1995; 154:964–967
5. Thoenes W, Storkel S, Rumpelt HJ, Moll R, Baum HP, Werner S. Chromophobe cell renal carcinoma and its variants: a report on 32 cases. *J Pathol* 1988; 155:277–287
6. Jasinski RW, Amendola MA, Glazer GM, Bree RL, Gikas PW. Computed tomography of renal

oncocytomas. *Comput Radiol* 1985; 9:307–314

7. Tikkakoski T, Paivansalo M, Alanen A, et al. Radiologic findings in renal oncocytoma. *Acta Radiol* 1991; 32:363–367
8. Quinn MJ, Hartman DS, Friedman AC, et al. Renal oncocytoma: new observations. *Radiology* 1984; 153:49–53
9. Davidson AJ, Hayes WS, Hartman DS, McCarthy WF, Davis CJ Jr. Renal oncocytoma and carcinoma: failure of differentiation with CT. *Radiology* 1993; 186:693–696
10. Kim JI, Cho JY, Moon KC, Lee HJ, Kim SH. Segmental enhancement inversion at biphasic multidetector CT: characteristic finding of small renal oncocytoma. *Radiology* 2009; 252:441–448
11. Ergen FB, Hussain HK, Caoili EM, et al. MRI for preoperative staging of renal cell carcinoma using the 1997 TNM classification: comparison with surgical and pathologic staging. *AJR* 2004; 182:217–225
12. Pretorius ES, Siegelman ES, Ramchandani P, Cangiano T, Banner MP. Renal neoplasms amenable to partial nephrectomy: MR imaging. *Radiology* 1999; 212:28–34
13. Semelka RC, Hricak H, Stevens SK, Finegold R, Tomei E, Carroll PR. Combined gadolinium-enhanced and fat-saturation MR imaging of renal masses. *Radiology* 1991; 178:803–809
14. Pedrosa I, Alsop DC, Rofsky NM. Magnetic resonance imaging as a biomarker in renal cell carcinoma. *Cancer* 2009; 115[suppl]:2334–2345
15. Oliva MR, Glickman JN, Zou KH, et al. Renal cell carcinoma: T1 and T2 signal intensity characteristics of papillary and clear cell types correlated with pathology. *AJR* 2009; 192:1524–1530
16. Pedrosa I, Sun MR, Spencer M, et al. MR imaging of renal masses: correlation with findings at surgery and pathologic analysis. *RadioGraphics* 2008; 28:985–1003
17. Jayson M, Sanders H. Increased incidence of serendipitously discovered renal cell carcinoma. *Urology* 1998; 51:203–205
18. Boorjian SA, Uzzo RG. The evolving management of small renal masses. *Curr Oncol Rep* 2009; 11:211–217
19. Harmon WJ, King BF, Lieber MM. Renal oncocytoma: magnetic resonance imaging characteristics. *J Urol* 1996; 155:863–867
20. Kondo T, Nakazawa H, Sakai F, et al. Spoke-wheel-like enhancement as an important imaging finding of chromophobe cell renal carcinoma: a retrospective analysis on computed tomography and magnetic resonance imaging studies. *Int J Urol* 2004; 11:817–824
21. Feinstein AR, Cicchetti DV. High agreement but low kappa. Part I. The problems of two paradoxes. *J Clin Epidemiol* 1990; 43:543–549
22. Abrahams NA, Tamboli P. Oncocytic renal neoplasms: diagnostic considerations. *Clin Lab Med* 2005; 25:317–339
23. Chao DH, Zisman A, Pantuck AJ, Freedland SJ, Said JW, Belldegrun AS. Changing concepts in the management of renal oncocytoma. *Urology* 2002; 59:635–642
24. Perez-Ordonez B, Hamed G, Campbell S, et al. Renal oncocytoma: a clinicopathologic study of 70 cases. *Am J Surg Pathol* 1997; 21:871–883
25. Sun MR, Ngo L, Genega EM, et al. Renal cell carcinoma: dynamic contrast-enhanced MR imaging for differentiation of tumor subtypes—correlation with pathologic findings. *Radiology* 2009; 250:793–802
26. Jinzaki M, Tanimoto A, Mukai M, et al. Double-phase helical CT of small renal parenchymal neoplasms: correlation with pathologic findings and tumor angiogenesis. *J Comput Assist Tomogr* 2000; 24:835–842
27. Choudhary S, Rajesh A, Mayer NJ, Mulcahy KA, Haroon A. Renal oncocytoma: CT features cannot reliably distinguish oncocytoma from other renal neoplasms. *Clin Radiol* 2009; 64:517–522
28. Beck SD, Patel MI, Snyder ME, et al. Effect of papillary and chromophobe cell type on disease-free survival after nephrectomy for renal cell carcinoma. *Ann Surg Oncol* 2004; 11:71–77
29. Ball DS, Friedman AC, Hartman DS, Radecki PD, Caroline DF. Scar sign of renal oncocytoma: magnetic resonance imaging appearance and lack of specificity. *Urol Radiol* 1986; 8:46–48
30. Krishnan B, Truong LD. Renal epithelial neoplasms: the diagnostic implications of electron microscopic study in 55 cases. *Hum Pathol* 2002; 33:68–79
31. Frank I, Blute ML, Cheville JC, Lohse CM, Weaver AL, Zincke H. Solid renal tumors: an analysis of pathological features related to tumor size. *J Urol* 2003; 170:2217–2220
32. Thompson RH, Kurta JM, Kaag M, et al. Tumor size is associated with malignant potential in renal cell carcinoma cases. *J Urol* 2009; 181:2033–2036
33. Mues AC, Landman J. Small renal masses: current concepts regarding the natural history and reflections on the American Urological Association guidelines. *Curr Opin Urol* 2010; 20:105–110
34. Chawla SN, Crispen PL, Hanlon AL, Greenberg RE, Chen DY, Uzzo RG. The natural history of observed enhancing renal masses: meta-analysis and review of the world literature. *J Urol* 2006; 175:425–431
35. Delongchamps NB, Galmiche L, Eiss D, et al. Hybrid tumour "oncocytoma-chromophobe renal cell carcinoma" of the kidney: a report of seven sporadic cases. *BJU Int* 2009; 103:1381–1384